Fast algorithm for spectral mixture analysis of imaging spectrometer data

Theo E. Schouten†, Maurice S. klein Gebbinck†, Z. K. Liu‡, S. W. Cen‡

†Katholieke Universiteit Nijmegen, Computing Science Institute,
Toernooiveld 1, 6525 ED Nijmegen The Netherlands
‡Department of Electronic Engineering and Information Science,
University of Science and Technology of China, Hefei 230026, China

ABSTRACT

Imaging spectrometers acquire images in many narrow spectral bands but have limited spatial resolution. Spectral mixture analysis (SMA) is used to determine the fractions of the ground cover categories (the end-members) present in each pixel. In this paper a new iterative SMA method is presented and tested using a 30 band MAIS image. The time needed for each iteration is independent of the number of bands, thus the method can be used for spectrometers with a large number of bands. Further a new method, based on K-means clustering, for obtaining endmembers from image data is described and compared with existing methods. Using the developed methods the available MAIS image was analyzed using 2 to 6 endmembers.

1 INTRODUCTION

Imaging spectrometers[15,16] acquire images simultaneously in many narrow spectral bands from visible to infrared. The imaging spectrometer data can be used[9] to determine the physical nature of the materials within the field of view qualitatively and estimate their abundances quantitatively. Previous research on imaging spectrometer data was on the identification of minerals[1,2] in semiarid and arid regions. Price and Westman[7] studied on the canopy chemistry with AIS data. Roberts et al.[9] studied the discrimination between green vegetation, nonphotosynthetic vegetation and soils in AVIRIS data. This previous research showed that imaging spectrometer data has big potentials in the analysis of the materials on the ground.

The signal received at an imaging spectrometer from a ground pixel presents the reflectance of the materials in the ground pixel. Spectral mixture analysis (SMA) is the methodology for decomposition of the mixture spectrum of each pixel, usually a linear mixture model[13,14] is used. The main ground cover types or classes in a remotely sensed image are called the image endmembers. Performing SMA for each pixel consumes a large amount of computer time and therefore it is important to develop faster algorithms for it. Also methods for obtaining endmembers from image data, which are fast and deliver good results, are needed.

In section 2 a new iterative algorithm for SMA is presented and results on test data, generated using intensity distributions obtained from a 30 channel image, using 3 and 4 endmembers are presented in section 3. This image was obtained from MAIS,[16] made in China. New methods of obtaining endmember spectra from image data, based on K-means clustering, are described in section 4. Endmember spectra obtained by the new and some existing methods are evaluated there by using them in the SMA of the MAIS image and comparing two error measures obtained from the SMA. In section 5 SMA results are presented using 2 to 6 endmembers, obtained using a K-means clustering method. In the last section conclusions are given.

2 FAST ITERATIVE ALGORITHM FOR SMA

The linear mixture model[5,13,9] assumes that each field within a ground pixel contributes to the signal received at the sensor an amount characteristic of its cover type and proportional to its area. The signal received for a pixel in the i'th band, s_i is then given by the following equation:

$$s_i = \sum_{j=1}^{c} f_j R_{ij} + e_i, \quad i = 1, 2, ..., n \tag{1}$$

where n is the total number of bands, R_{ij} is the reflectance of the jth endmember in the ith band, f_j is the fraction of the ground pixel covered by endmember j, e_i is the error in the ith band, and c is the total number of endmembers in the image.

Rewriting equation 1 into vector matrix notation ($S = RF + E$) a least squares solution, minimizing $\|E\|^2$, can be given as:

$$F_{ls} = (R^T R)^{-1} R^T S \tag{2}$$

but this does not in general satisfy the conditions to be posed on F:

$$\sum_{j}^{c} f_j = 1 \quad and \quad 0 \leq f_j \quad j = 1, ..., c \tag{3}$$

Using linear algebra[3,11,4] the optimum solution can be obtained, but numerical methods are needed (possible using exhaustive search through a range of possibilities) to ensure the positivity constraints on f_j. Because of the large amount of computer time needed, an iterative method was developed to find the optimum solution.

A cost function is defined as:

$$\|E(F)\|^2 + g1(F) + g2(F) \tag{4}$$

$$g1(F) = \sum_{j=1}^{c} (if \ f_j < 0 \ then \ f_j^2 \ else \ 0) \tag{5}$$

$$g2(F) = (\sum_{j=1}^{c} f_j - 1)^2 \tag{6}$$

and minimized with respect to f_j starting from the least squares solution with a gradient descent method:

$$f_j^{(k+1)} = f_j^{(k)} - \alpha_0 \frac{\partial \|E\|^2}{\partial f_j} - \alpha_1 \frac{\partial g_1(F)}{\partial f_j} - \alpha_2 \frac{\partial g_2(F)}{\partial f_j} \tag{7}$$

The partial differentials are:

$$\frac{\partial \|E\|^2}{\partial f_j} = \frac{\partial \sum_{i=1}^{n} e_i^2}{\partial f_j} = \sum_{i=1}^{n} 2e_i \frac{\partial e_i}{\partial f_j} = -\sum_{i=1}^{n} 2e_i R_{ij} \tag{8}$$

$$\frac{\partial g1(F)}{\partial f_j} = \begin{cases} 2f_j, & f_j < 0 \\ 0, & f_j \geq 0 \end{cases} \tag{9}$$

$$\frac{\partial g2(F)}{\partial f_j} = 2(\sum_{j=1}^{c} f_j - 1) \tag{10}$$

In equation (8) there are n multiplications and additions for each endmember and in imaging spectrometer data the number of bands n can be from several tens to several hundreds, much more then the number of endmembers c. Fortunately we found that it can be rewritten, using $R^T R F_{ls} = R^T S$ obtained from equation (2), as:

$$\frac{\partial \|E\|^2}{\partial F} = -2R^T E = -2R^T(S - RF) = 2R^T RF - 2R^T S = 2R^T R(F - F_{ls}) \tag{11}$$

$$\frac{\partial \|E\|^2}{\partial f_j} = \sum_{p=1}^{c} m_{jp}(f_p - f_{ls_p}) \; with \; m_{jp} = 2\sum_{i=1}^{n} R_{ij} R_{ip} \tag{12}$$

Because $M = R^T R$ is independent from the iterations the time complexity of an iteration step for each endmember is thus proportional to c, the number of endmembers. Each iteration step can thus be performed very fast and if the number of needed iteration steps is low (as will be shown to be the case for the studied examples in section 3) the whole SMA method will be fast.

3 TEST OF FAST ITERATIVE ALGORITHM

The intensities of the endmembers for this test were taken from an image of 512X475 pixels (showing the Yellow River Valley in the Ganshu province in China) from MAIS (Modular Airborne Imaging Spectrometer) made in China. It has 30 bands from visible to infrared, the resolution of the bands is 20 nm and each pixel corresponds to $20X20m^2$ of the earth surface. The grey level of pixels is from 0 to 255. Three endmember pixels were chosen corresponding to water, vegetation and soil based on visual inspection. For each endmember some 16 area's of 5 by 5 pixels were selected by a computer method[10] from the image.

The signal S for each of the 16384 test pixels was generated in the following way. One of the f_j's (rotating when going from pixel to pixel) was taken as an uniform random number between 0 and 1, another as an uniform random number between 0 and 1 minus the first f and the last one as 1 minus the sum of the other two f's. For the endmember matrix random multivariate gaussians were used according to the mean vectors and covariance matrices of the example sets of the endmembers. This models both matrix R and a contribution to the error vector E. Further a random gaussian of mean 0.0 and σ of 2.0 was added to each channel to model sensor noise. Finally the intensities were rounded to the nearest integer and truncated to the range 0 to 255.

After some experimentation the following values for the α's were used: $\alpha_0 = 0.1/(256 * 256 * n)$, $\alpha_1 = 0.25$ and $\alpha_2 = 0.5/c$. In figure 1 the following error measures are shown:

$$\begin{aligned}
Energy - error &= \sqrt{\frac{\sum_{p=1}^{N}\sum_{i=1}^{n} e_{pi}^2}{nN256^2}} \\
Sumf - error &= \sqrt{\frac{\sum_{p=1}^{N}(\sum_{j=1}^{c} f_{pj} - 1)^2}{N}} \\
F - error &= \sqrt{\frac{\sum_{p=1}^{N}\sum_{j=1}^{c}(f_{pj} - ft_{pj})^2}{cN}} \\
Condition - error &= fraction\ of\ f_j's\ not\ in\ range\ 0\ to\ 1
\end{aligned}$$

Here N is the number of test pixels and ft is the true fraction of the endmember. The errors decrease except the energy error for which the least squares method finds the minimum value not taken the conditions on f into

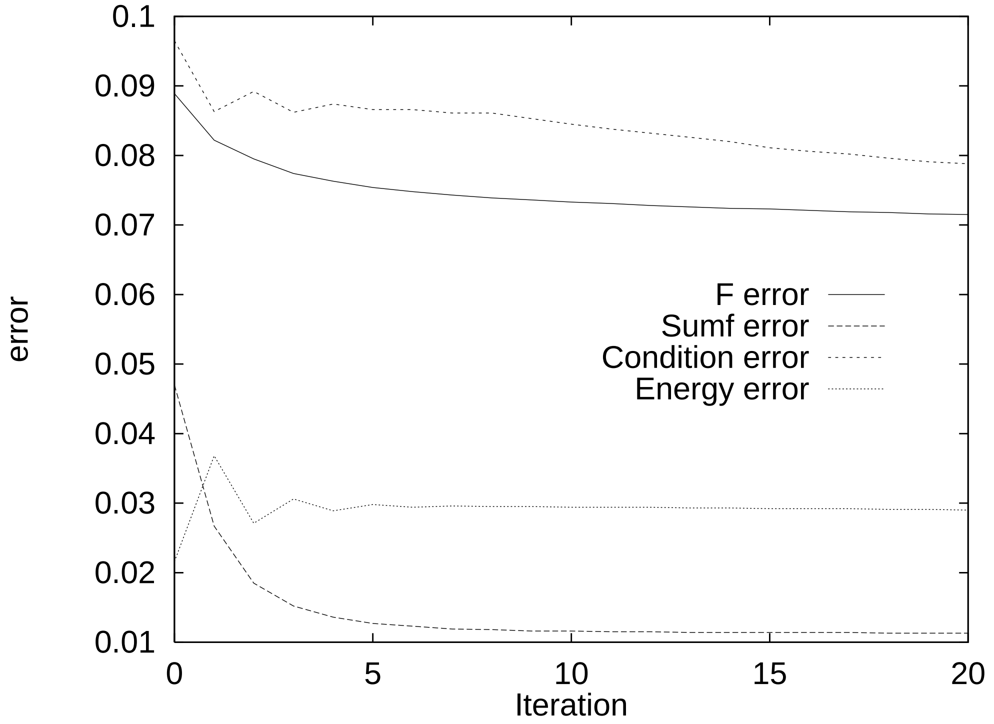

Figure 1: Errors vs number of iterations

account. Histograms of $\sum_{j=1}^{c} f_j$ and of $(f_j - ft_j)$ are shown in figure 2. The sum of the f's become closer to 1 and the errors on f decrease.

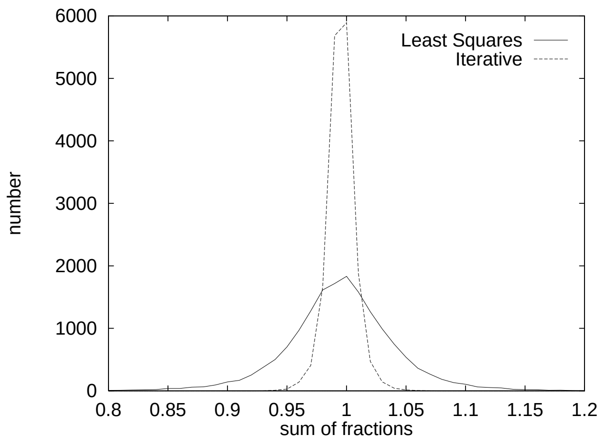

(a) Sum of f

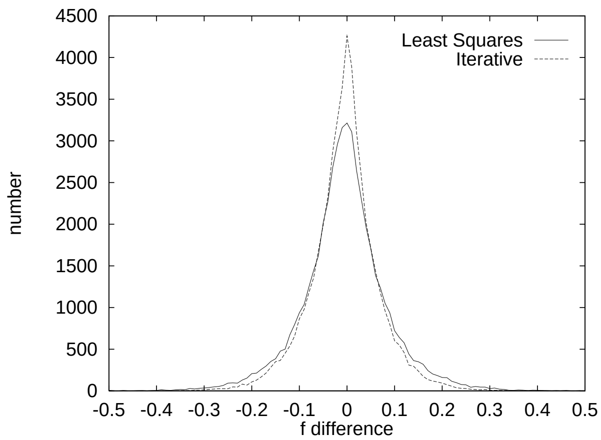

(b) f difference

Figure 2: Histograms of $\sum_{j=1}^{c} f_j$ and of $(f_j - ft_j)$ for 3 endmembers

To further test the new SMA method a fourth endmember was added for which the extra endmember, found in section 5 when determining 4 endmembers from the MAIS image, was taken. Its covariance matrix was set

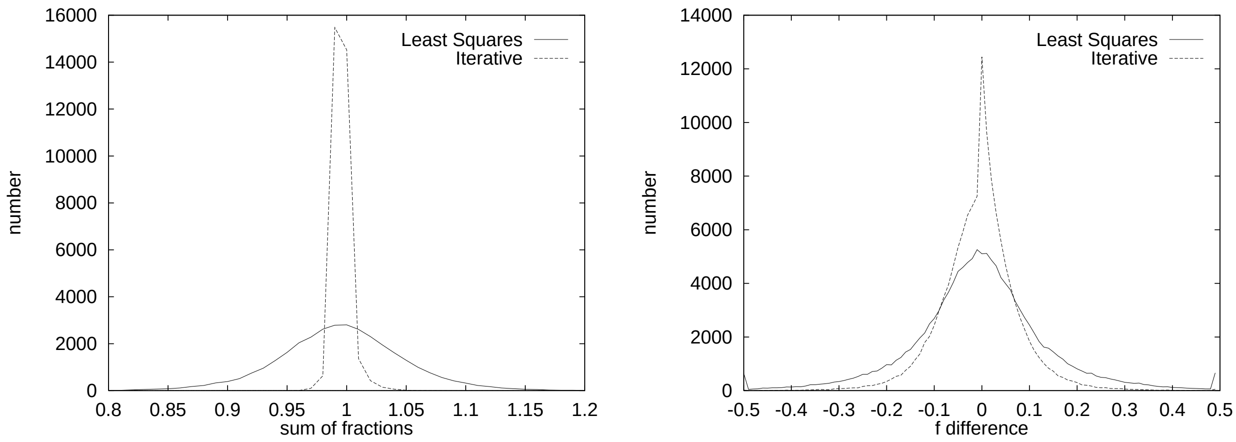

(a) Sum of f (b) f difference

Figure 3: Histograms of $\sum_{j=1}^{c} f_j$ and of $(f_j - ft_j)$ for 4 endmembers

to the average of the covariance matrices of the first two endmembers. A test set of 32768 pixels was generated in a similar way as for 3 endmembers, and the $Sumf - error$ and the $F - error$ of its SMA analysis are shown in figure 3. The improvement on the errors is larger than when using 3 endmembers.

4 SELECTION OF ENDMEMBERS

Different methods for obtaining endmembers from an image exist. The quality of those endmembers could be judged by comparing them to known spectra of ground covers if they are available. Another method of evaluating the quality is by performing the spectral mixture analysis on a whole image and calculating the error measures $Energy - error$ and $Sumf - error$ as defined in the previous section. In table 1 these errors are shown for the endmember obtained with the methods described in this section using the fast iterative algorithm for 20 iterations on the MAIS image.

	$Energy - error$	$Sumf - error$
Visual	0.0895	0.0462
Visual + selection	0.0869	0.0477
PCA	0.1641	0.0485
K-means	0.0787	0.0317
K-means + $f > 85\%$	0.0751	0.0383
K-means + area's	0.0726	0.0344

Table 1: $Energy - error$ and $Sumf - error$ for different endmembers

In the previous section already two methods for the selection of endmembers were used: visual selection of single pixels and selection of area's using those single pixels as start values followed by averaging the intensities of the obtain pixels. In figures 4(a) and 4(b) the spectra of the endmembers so obtained from the MAIS image are shown. As expected there is a relatively small change in intensities but the form of the spectra is the same. As shown in table 1 the $Energy - error$ decreases and the $Sumf - error$ increases by a small amount when

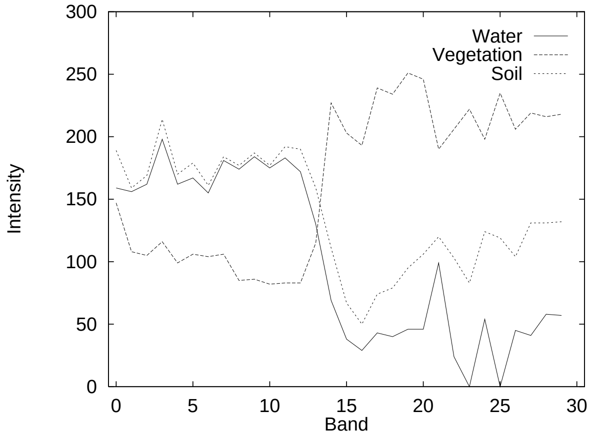

(a) Visual

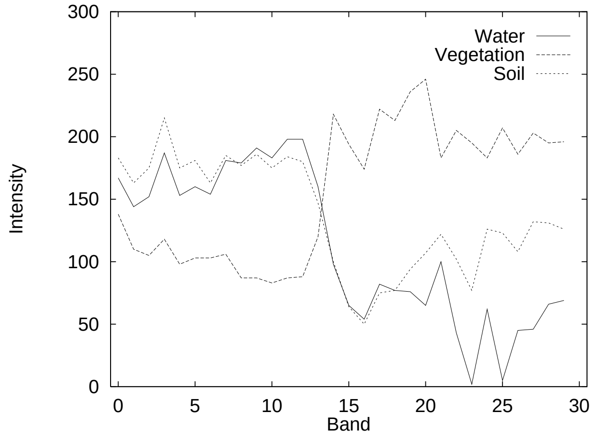

(b) Visual + selection

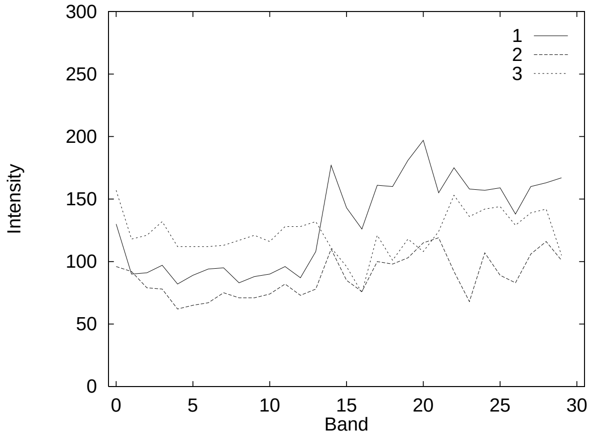

(c) Principal Component Analysis

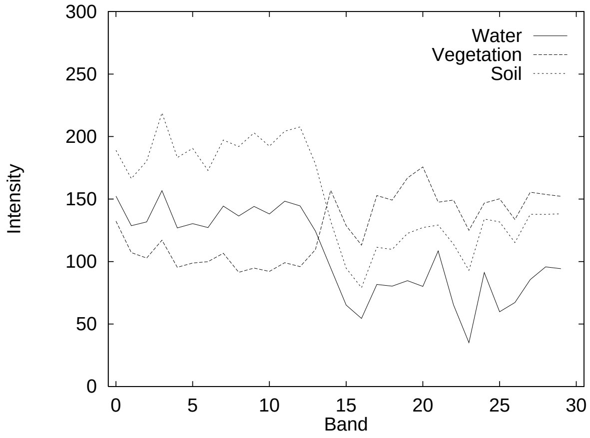

(d) K-means

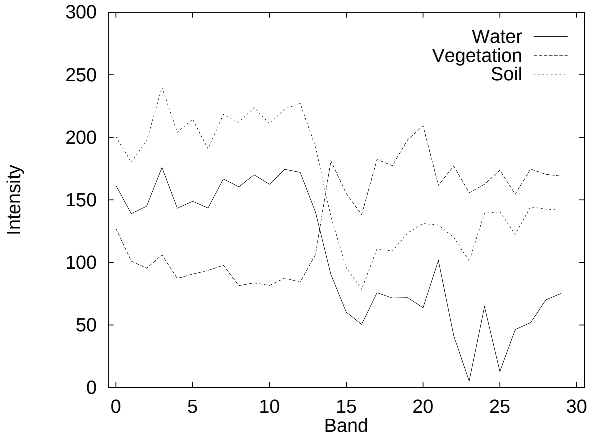

(e) K-means + $f > 85\%$

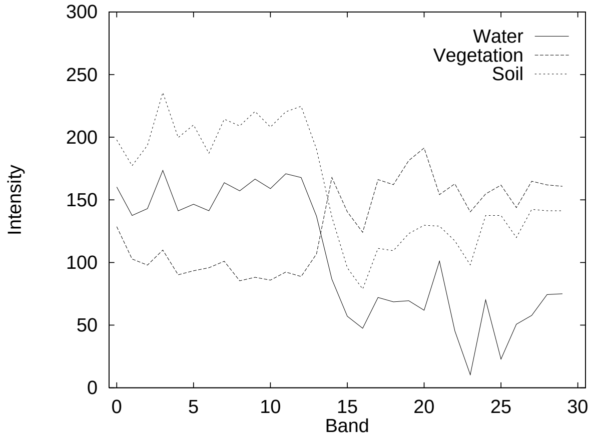

(f) K-means + area's

Figure 4: Spectra of endmembers

using the selection method.

A method for automatically choosing the endmembers as done by[12] and[3] is using Principal Component Analysis. The so obtained endmembers are shown in figure 4(c), the distributions are more or less flat and close together. The obtained $Energy - error$ is much larger than for the visual methods.

As a new method for automatically determining the endmembers from image data, we tried simple K-means clustering. A fixed number of clusters is taken and initial cluster center intensities are defined in some way. Then each pixel is assigned to the cluster to which it is closest in intensity (minimal $\|S_p - S_c\|^2$ with S_p the intensities of the pixel and S_c the intensities of the center of cluster c). For each cluster new center intensities are then calculated as the average of the intensities of the pixels assigned to that cluster. The process of assignment of pixels and recalculation of the centers is then repeated until there is no change in center intensities and the final cluster centers are taken as the endmembers.

It appeared that for all initial cluster values tried, the clustering terminated after 20 to 35 iterations. Nearly the same endmembers (root mean square difference between intensities less than 0.4) are produced taking as initial cluster centers respectively the $Visual$ or $Visual + selection$ endmembers, flat distributions at intensity values of 64, 128 and 192 or 127, 128 and 129, or most of the random selection of 3 pixels in the image. The endmembers when starting from the $Visual$ endmembers are shown in figure 4(d), they look more like the $Visual$ endmembers (compared to the PCA end members) but with intensities closer together. As shown in table 1 both errors are lower for this set of $K - means$ endmembers than for the 3 previous ones.

When initializing with the PCA endmembers, flat spectra at 227, 228 and 229, or some of the random selection of pixels, another set of endmembers was found. Its rms difference with the $K - means$ endmember set was 15.2 and the SMA errors were higher (0.0798 and 0.0320). Therefore this set was not further considered.

Two methods were tried to improve on the $K - means$ endmembers by selecting relatively pure pixels from the image. In the first one the fast iterative algorithm for SMA was performed on the whole image and pixels having one of the f's above 85% were selected. In the second one area's in the image of 10 by 10 pixels all belonging to the same cluster were determined and the 8 by 8 inner pixels of those area's were selected. The selected pixels were then averaged to obtain the new endmembers which are shown in figures 4(e) and 4(f). These endmembers are closer to the $Visual$ endmembers. Table 1 shows that these selection methods decrease the $Energy - error$ but increase the $Sumf - error$ by a small amount.

5 USING DIFFERENT NUMBER OF ENDMEMBERS

The K-means clustering method described in section 4 can be used to determine any number of endmembers from the image data. Taking as initial cluster centers flat spectra at intensity levels of $i/c + 1$ with $i = 1...c$ and c the number of endmembers, K-means clustering endmembers were determined for 2 to 6 endmembers and improved by the $area's$ method. The so obtained endmembers are shown in figures 5(a) to 5(d) except for 3 endmembers which was shown in figure 4(f), in table 2 the corresponding SMA errors are given.

Number of endmembers	$Energy - error$	$Sumf - error$
2	0.0921	0.0312
3	0.0726	0.0344
4	0.0643	0.0242
5	0.0754	0.0467
6	0.0990	0.1222

Table 2: Errors for different number of endmembers

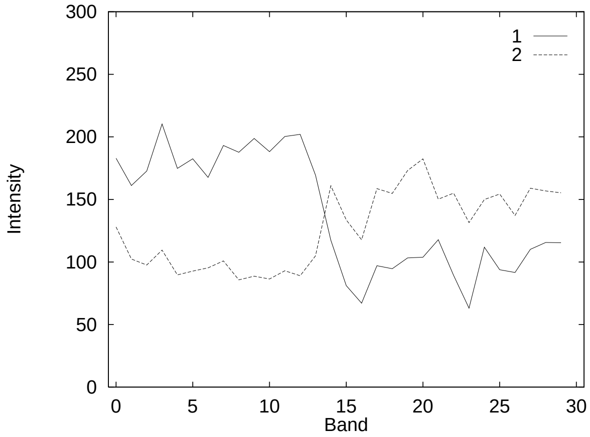

(a) 2

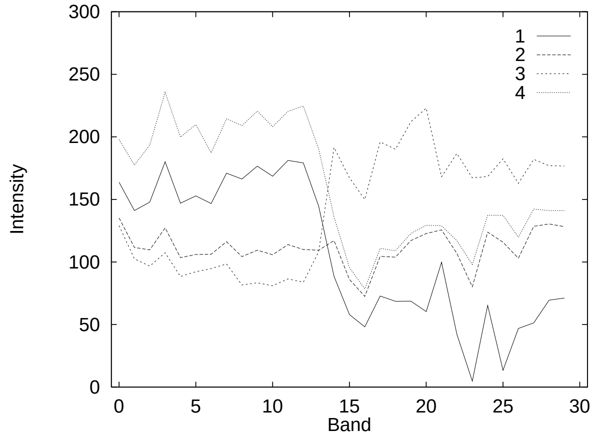

(b) 4

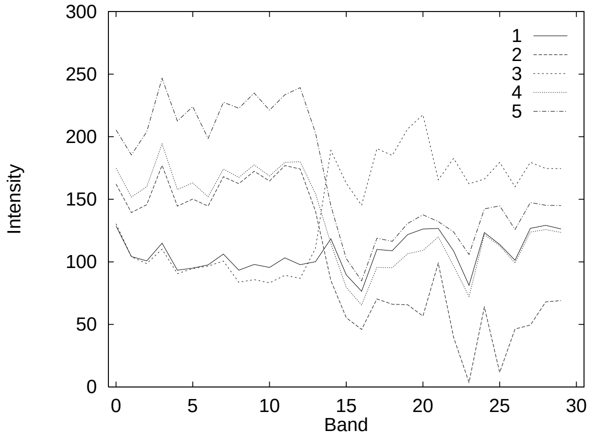

(c) 5

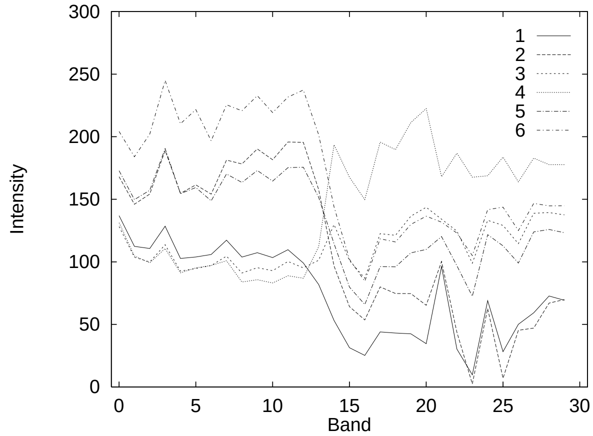

(d) 6

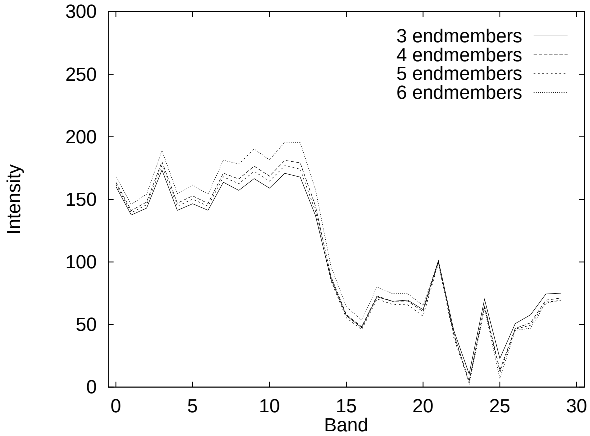

(e) Water comparison

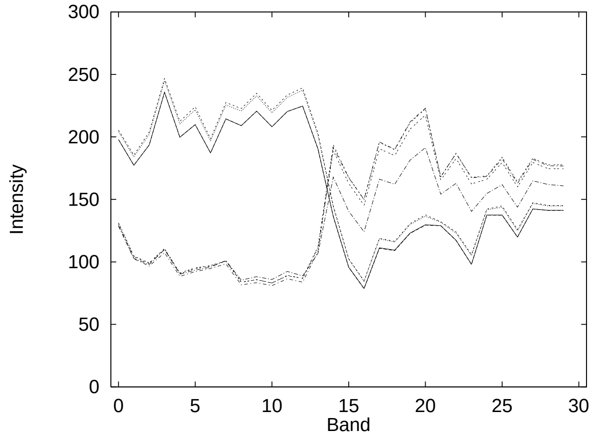

(f) Vegetation and soil comparison

Figure 5: Endmember spectra and comparison for different number of endmembers

The lowest errors are obtained with 4 endmembers, thus that seems to be the optimal case. Comparing the endmembers one notice that the water, vegetation and soil endmembers from the 3 endmembers case appear more or less in the same form in the 4, 5 and 6 endmembers cases. This is clearer shown in figures 5(e) and 5(f). It is an indication that they present real ground covers present in the image.

Comparing the 4 with the 3 endmembers one notice besides the hardly changed water, vegetation and soil spectra an additional more or less flat spectrum. The results of SMA of the 3 resp. 4 endmembers into the 4 resp. 3 endmembers is shown in table 3. As expected the 3 endmembers can be better described as combinations of the 4 endmembers than the other way around. In the SMA of 3 endmembers the water contains 11% and the vegetation 31% of the extra flat endmember and in the SMA of the 4 endmembers the latter is described as consisting of 41% water and 57% vegetation. It would be interesting to analyze this further and to compare the endmembers with known spectra of ground covers.

	SMA of 3 endmembers				SMA of 4 endmembers		
	Water	Vegetation	Soil	Extra	Water	Vegetation	Soil
Water	0.888	-0.001	-0.001	0.110	1.003	-0.004	0.008
Vegetation	-0.001	0.686	-0.001	0.313	-0.013	1.044	-0.007
Soil	0.000	0.001	0.999	0.000	0.002	-0.000	0.998
Extra					0.414	0.575	-0.003
$Energy - error$	0.0066				0.0350		
$Sumf - error$	0.0031				0.0144		

Table 3: SMA of 3 (resp. 4) endmember spectra into 4 (resp. 3) endmembers

6 CONCLUSIONS

A new method for spectral mixture analysis of imaging spectrometer data has been developed and tested using data from a 30 channel image of the MAIS spectrometer. The method is iterative and fast because the time needed for each iteration step for each endmember is proportional to the number of endmembers, independently of the number of bands in the image. It decreases the difference between the found and true fractions of the endmembers compared to the least squares method.

New methods, based on K-means clustering, have been developed for obtaining endmembers from image data. With the so obtained endmembers for the MAIS image lower SMA error values were obtained than with endmembers obtained with existing methods. These SMA errors describe the difference between the measured intensities of pixels and the intensities calculated from the endmembers and the deviation of the sum of the fractions from 1.

The MAIS image was analyzed using the developed methods using 2 to 6 endmembers, using 4 endmembers appeared to give the lowest SMA errors. The endmembers obtained when using 3 endmembers appear relatively unchanged when going to 4, 5 and 6 endmembers, an indication that they are really fundamental covers in the MAIS image. It would be interesting to compare the obtained endmembers with spectra from pure ground covers when they are available.

7 REFERENCES

[1] R.N. Clark, A.J. Gallagher, G.A. Swayze. Material absorption and band depth mapping of imaging spectrometer data using a complete band shape least squares fit with library reference spectra. *Proc. 2nd Airborne Visible/infrared Imaging Spectrometer(AVIRIS) Workshop (R. O. Green, Ed.)*, Pasadena, CA, 4-5 June, pp. 178-186 (1990).

[2] W. Collins, S.H. Chang, G. Raines, F. Canney, R. Ashley. Airborne biophysical mapping of hidden mineral deposits. *Econ. Geol* 78, pp. 737-828 (1983).

[3] A.M. Cross, J.J. Settle, N.A. Drake, R.T.M. Paivinen. Subpixel measument of tropical forest cover using AVHRR data, *International Journal of Remote Sensing*, 12: 1119-1129, 1991.

[4] M.S. klein Gebbinck, T.E. Schouten. Decomposition of mixed pixels. *Image and Signal Processing for Remote Sensing II* Jacky Desachy, ed., Proc. SPIE 2579, (1995)

[5] F.A. Kruse et al. The Spectral imaging Processing System(SIPS) Interactive Visualization and Analysis of Imaging Spectrometer Data. *Remote Sensing of Environment*, Vol. 44, pp. 145-163 (1993).

[6] LIU, Z. K., and XIAO, J. Y., 1991, Classification of Remotely Sensed Image Data Using Artificial Neural networks, *International Journal of Remote Sensing*, Vol. 12, No. 11.

[7] G.V. Price, W.E. Westman. Toward detecting shrubland canopy chemistry with AIS data. *Proc. 3rd Airborne Imaging Spectrometer Data Analysis Workshop*, Pasadena, CA, 2-4 June, pp. 91-99 (1987).

[8] N.A. Quarmby et al. Linear mixture modelling applied to AVHRR data for crop area estimation. *International Journal of Remote Sensing*, Vol. 13, No. 3, 415-425 (1992).

[9] D.A. Roberts, M.O. Smith, J.B. Adams. Green Vegetation, Nonphotosynthetic Vegetation, and Soils in AVIRIS Data. *Remote Sensing of Enviroment*, Vol. 44, pp. 255-269 (1993).

[10] Theo E. Schouten, Maurice S. klein Gebbinck. Quality Measures for Image Segmentation using Generated Images. *Image and Signal Processing for Remote Sensing II* Jacky Desachy, ed., Proc. SPIE 2579: 411-422 (1995).

[11] J.J. Settle, N.A. Drake. Linear mixing and the estimation of ground cover proportions, *International Journal of Remote Sensing*, 14: 1159-1177, 1993.

[12] M.O. Smith, P.E. Jonhson, J.B. Adams. Quantitative determination of mineral types and abundances from reflectance spectra using principal component analysis. *Proc. 15th Lunar Planet. Sci. Conf., J. Geophys. Res.*, Vol. 80, Part 2, pp. C797-C804 (1985).

[13] M.O. Smith, S.L. Ustin, J.B. Adams, A.R. Gillespie. Vegetation in Deserts: I. A Regional Measure of Abundance from Multispectral Images. *Remote sensing of Environment*, Vol. 31 pp. 1-26 (1990).

[14] M.O. Smith, S.L. Ustin, J.B. Adams, A.R. Gillespie. Vegetation in Deserts: II. Environmental Influences on Regional Abundance. *Remote sensing of Environment*, Vol. 31 pp. 1-26 (1990).

[15] G. Vane et al. The Airborne Visible/Infrared Imaging Spectrometer(AVIRIS). *Remote Sensing of Environment*, 44:127-143, 1993.

[16] Y.Q. Xue. The Technical Development of Airborne Scan Imaging Systems, *Journal of Infrared and Millimeter Waves (China)*, 11: 168-191, 1992.